



# Complex modulus of cement-bitumen treated materials produced with different reclaimed asphalt gradations

Chiara Mignini · Fabrizio Cardone · Andrea Graziani

Received: 6 April 2022 / Accepted: 14 July 2022  
© The Author(s) 2022

**Abstract** The increasing attention over cold recycling technologies as sustainable paving solutions requires a proper characterisation in terms of complex modulus for supporting the pavement design. Among cold recycled materials, cement bitumen treated materials (CBTM) benefit from the presence of both bituminous and cementitious binders. This research aims at characterising the complex modulus of CBTM mixtures produced with three different gradations, modified bitumen emulsion and two types of cement. The complex modulus measurements were modelled considering the usual viscous dissipation behaviour, linked to the bituminous component of the mixtures, along with a time- and temperature-independent dissipation component. The results showed that both the aggregate skeleton and the composition of the fine aggregate matrix affected the rheological behaviour. Furthermore, the role played by the aged binder contained in the reclaimed asphalt aggregate was highlighted by the parameters of the rheological model.

**Keywords** Cold recycling · Bitumen emulsion · Complex modulus · Gap-graded gradation · Thermo-rheological modelling

---

C. Mignini · F. Cardone · A. Graziani (✉)  
Dipartimento di Ingegneria Civile Edile e Architettura,  
Università Politecnica Delle Marche, Via Breccie Bianche,  
60131 Ancona, Italy  
e-mail: a.graziani@univpm.it

## 1 Introduction

The global concern over the sustainability of the built environment is pushing policy makers towards new strategies for implementing high-quality recycling and reducing carbon and environmental footprints [1]. In pavement engineering, cold recycling techniques allow the reuse of high amounts of reclaimed asphalt (RA), generally between 50 and 100% of the total aggregate blend, and are carried out at ambient temperature. This may save up to 50% of fuel consumption compared to traditional hot mix asphalt (HMA) technologies [2, 3] and reduce greenhouse gases and pollutants emissions [4–7].

Cold recycled material (CRM) mixtures are normally produced using continuous (dense-graded) gradations [8–12]. However, several studies have shown that discontinuous (gap-graded) gradations and higher content of fines may improve the compactability and the mechanical behaviour of the mixtures [13–16]. As regards the binding agents, bitumen emulsion or foamed bitumen are often used in combination with Portland cement or other chemical additives, such as lime. In this respect, promising results have been obtained using modified emulsions [17–20] and non-Portland cements [21–23].

Optimising the composition of CRM mixtures is the first step towards their wider implementation as a replacement for conventional HMA mixtures. In order to apply mechanistic-empirical design procedures to



pavements including cold recycled material (CRM) layers [24], it is imperative to characterize their stiffness properties. This requires different testing and modelling approaches, depending on the composition of the mixture, in particular, the type and amount of binding agents. If cold recycling is carried out using only Portland cement, stiffness can be characterised using the approach employed for cement-treated materials (CTM) [25]. If bitumen is the main recycling agent a bitumen stabilised materials (BSM) is obtained, whose stiffness characterisation must take into account stress-dependency [26, 27]. In pavement design, both CTM and BSM layers are considered time- and temperature-independent, and therefore the measurement of stiffness at different temperatures and loading frequencies is normally not of concern. On the other hand, cold recycled asphalt (CRA) and cement-bitumen treated materials (CBTM) mixtures show a typical frequency- and temperature-dependent stiffness behaviour [28–32]. Therefore, their stiffness can be measured using complex modulus tests and modelled using linear viscoelastic (LVE) models [33, 34]. The same experimental procedures and thermo-rheological models developed for conventional HMA mixtures are normally applied for CRA and CBTM mixtures [33, 34]. However, these mixtures have some peculiarities that must be properly considered, like the interaction between the heavily aged RA binder and the fresh bitumen used as binding agent.

In this research we focused on the measurement and modelling of the complex modulus behaviour of CBTM mixtures produced with latex-modified bitumen emulsion and cement. Our main objective was to evaluate the effect of different grading curves on the complex modulus behaviour. The effects of RA content and cement type were also investigated. To tackle this objective, we applied a rheological modelling approach specifically developed for CBTM mixtures, which considers also non-viscous dissipation mechanisms. The paper is organised as follows: Sect. 2 presents a short review of current approaches for modelling the complex modulus of CBTM mixtures; Sect. 3 provides information on the tested mixtures, the complex modulus testing procedure and the proposed rheological modelling approach; Sect. 4 describes the experimental and model fitting results and Sect. 5 discusses the values of some rheological parameters and compares the results with those obtained from the review.

## 2 Literature review

This review focuses on studies where the complex modulus of CBTM mixtures, or at least the stiffness modulus (i.e. the absolute value of the complex modulus, also known as dynamic modulus), was measured and modelled applying analogical or mathematical models. Table 1 summarises the literature sources and includes information on the composition of the mixtures, the curing protocol and the rheological modelling approach. The RA content of those mixtures varied between 20 and 100% and the fines content varied between 1.8 and 9.6%. As regards their volumetric properties, the air voids content varied between 8.9 and 18.0%. As regards the binding agents, the dosage of fresh bitumen (residual from the emulsion or foamed) varied between 1.2 and 3.8%, whereas the dosage of cement varied between 1.0 and 4.0%. The dosages of fresh bitumen and cement are reported in Fig. 1, where the tentative composition limits for the four families of CRM mixtures described in the Introduction are also outlined.

In all the literature sources, the time–temperature superposition principle (TTSP) was applied to obtain the master curves of the stiffness modulus. To compare among different papers, we shifted the master curves to the same reference temperature  $T_{\text{ref}} = 25$  °C using the reported shift factors (Fig. 2). Only the master curves of mixtures from 19 to 28 (Table 1) refer to  $T_{\text{ref}} = 21.1$  °C because the shift factors values were not provided [33]. As can be observed, the curves show a high dispersion, which is not surprising, given the wide range of compositions, voids content and curing conditions. The equilibrium moduli ( $E_e$ ) and glassy moduli ( $E_g$ ) reported in the literature sources are also listed in the last two columns of Table 1. The dispersion is particularly high for  $E_e$  that varies between  $10^{-5}$  and 1479 MPa. Such a dispersion is also due to the calibration of the adopted models. In fact, the rheological models' equations were fitted within the range of reduced frequencies covered by the experimental data. Therefore, we may expect lower precision when predicting the behaviour of the mixtures at the asymptotic conditions represented by  $E_e$  and  $E_g$ .



**Table 1** Summary of CRM mixtures considered in the complex modulus review

References	Mix ID	RA (%)	NMAS (mm)	Fines (%)	Bitumen type	Bitumen (%)	Cement (%)	B/C	Voids (%)	Curing	Model	$E_c$ (MPa)	$E_g$ (MPa)
Cardone et al. [35]	1–2	50	31.5	1.8–2	E	1.8	1.0	0.9–1.8	NA	20 °C–28 days	Sigmoidal-4 parameters	750	11,912
Godenzoni et al. [36]	3–4	50	20	11.7	F	3.0	1.5	2.0	10.0	40 °C–14 days	Huet-Sayegh	112–158	5076–5295
Dolzycki et al. [12]	5–13	70	40	5.0	E	2–6	2–6	0.3–3.0	14.2–18	20 °C–1.5 years	Sigmoidal-4 parameters	11–750	7642–12,394
Gandi et al. [37]	14–17	50–100	14–24	2.3–5.0	E	1.8	1.0	1.8	8.9–14.4	38 °C–10 days	2S2PID	80–320	7900–12,625
Lin et al. [38]	18	100	26.5	2.1	E	1.8	2.0	0.9	NA	65 °C–21 days	Sigmoidal-4 parameters	200	23,418
Schwartz et al. [33]	19–23	NA	NA	NA	F	NA	NA	NA	NA	field→1 year	Sigmoidal-4 parameters	0.4–622	2918–11,924
	24–28	NA	NA	NA	E	NA	NA	NA	NA	field→1 year	Sigmoidal-4 parameters	0.5	10,388–27,253
Buczyński and Iwański [39]	29–32	20–80	31.5	8.0	F	2.5	2.0	1.3	12.0	20 °C–28 days	Sigmoidal-5 parameters	1479	13,490
Graziani et al. [40]	33	50	31.5	9.5	E	1.8	2.0	0.9	12.4	40 °C–14 days	2S2PID	1479	13,490
Kuchiishi et al. [41]	34	68	20	4.0	E	3.0	2.0	1.5	NA	40 °C–28 days	Sigmoidal-4 parameters	10 <sup>-5</sup>	10,889
	35	68	20	6.0	F	3.0	2.0	1.5	NA	40 °C–28 days	Sigmoidal-4 parameters	10 <sup>-3</sup>	13,335
Graziani, Mignini, et al. [34]	36	33	63	6.2	E	1.8	2.0	0.9	17.5	Field—10 years	Huet-Sayegh-HY	645	7484
Graziani, Raschia, et al. [31]	37	94	31.5	9.6	E	3.0	1.5	2.0	15.0	25 °C–14 days + 40 °C–14 days	Huet-Sayegh-HY	196	9369
Ferrotti et al. [18]	38	88	31.5	5.1	E	2.7	2.0	1.4	14.3	Field—194	Huet-Sayegh-HY	833	13,583

NA, information not available,  $E_c$  bitumen emulsion,  $F$  foamed bitumen



### 3 Materials and methods

#### 3.1 Materials

The RA aggregate had a nominal maximum aggregate size (NMAS) of 16 mm (RA 0/16). In the laboratory, two fractions were further separated using the 2 mm sieve: RA 0/2 and RA 2/16. The virgin fine aggregate was crushed limestone sand with NMAS of 2 mm, and the filler was a finely ground limestone dust. Table 2 lists the main properties of the aggregates and Fig. 3a depicts their gradations. For the RA aggregate, the so-called “black curve” is reported. The bitumen

emulsion was a commercial cationic slow-setting type, specifically designed for cold recycling applications, and classified C 60 BP 10 according to the European standard EN 13808. The emulsion was modified with Styrene-Butadiene-Rubber latex, and its residual bitumen content was 60%. Two types of cementitious binders were used, coded C2 and C3 [23], both are characterised by high compressive strength after 28 days according to EN 196-1.

#### 3.2 Mixtures

The mixtures tested in this research were designed to be used in binder courses of medium-to-high traffic roadways. Three gradations with NMAS of 16 mm (Fig. 3b) were evaluated:

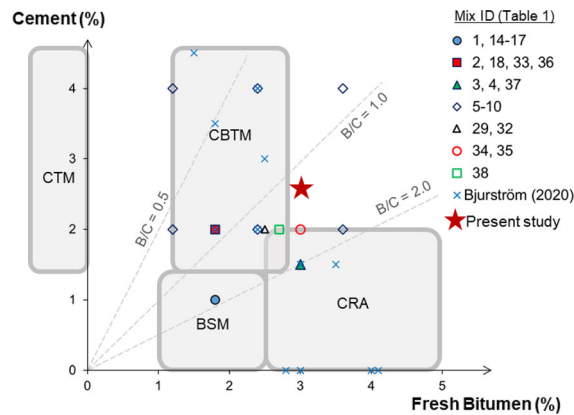


**Fig. 1** Composition of the CRM mixtures listed in Table 1 and identification of CRM mixtures families

- A dense-graded gradation (DG) derived from the Fuller-Thompson curve with exponent 0.45. The RA aggregate content was 80%;
- A gap-graded gradation (GG) whose coarse fraction (particles retained on the 2 mm sieve) was constituted by the RA 2/16, whereas the fine fraction (particles passing to the 2 mm sieve) was natural sand and filler;
- A gap-graded gradation, with RA aggregate content of 95% (GGRA).

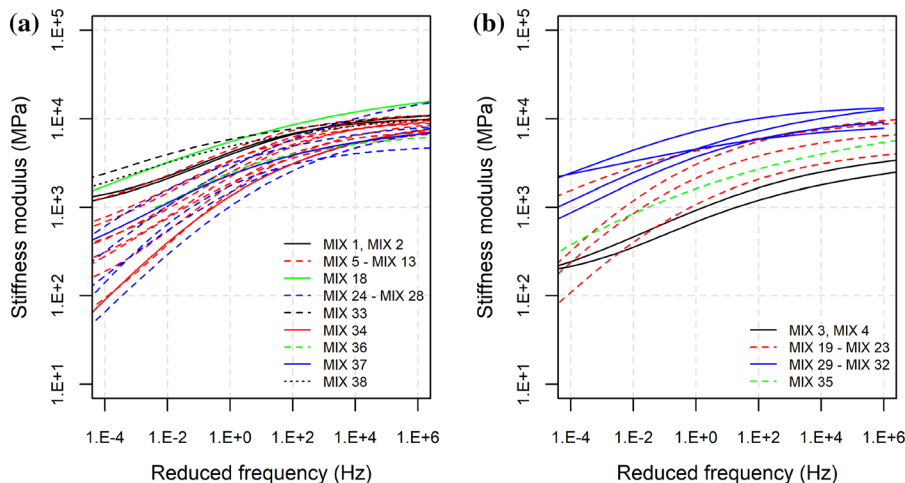


**Fig. 2** Stiffness modulus master curves at the reference temperature  $T_{ref} = 25 \text{ }^\circ\text{C}$  for the mixtures listed in Table 1: **a** mixtures produced with bitumen emulsion; **b** mixtures produced with foamed bitumen



**Table 2** Main properties of the aggregates

Property	Standard	RA 0/16	RA 0/2	RA 2/16	Sand	Filler
NMAS (mm)	EN 933-1	16	2.0	16	2.0	0.125
Passing the 0.063 sieve (%)	EN 933-1	5.6	16.9	0	12.2	45.3
Particle density (kg/m <sup>3</sup> )	EN 1097-6	2482	2424	2550	2732	2650
Water absorption (%)	EN 1097-6	1.14	1.32	1.14	1.50	
Soluble binder content (%)	EN 12697-1	5.0	8.3	3.2		
Rigden voids (%)	EN 1097-4					23.8
Blaine finesses (cm <sup>2</sup> /g)	EN 196-6					3400

The DG gradation fits within the gradation limits specified by Italian technical guidelines for cold recycling [42, 43]. The two gap-graded gradations fit within the limits specified by Italian technical guidelines for stone mastic asphalt (hot) mixtures [43]. Figure 4a shows that the GG and GGRA gradations had the same coarse RA aggregate skeleton but different compositions in terms of fine aggregate. The GG gradation comprised only virgin fine aggregate, whereas the GGRA gradation comprised mostly fine RA aggregate particles. Figure 4b shows the relative volume fractions of the fresh bitumen from the emulsion and the aged bitumen from RA 2/16 and RA 0/2. It is highlighted that the fine fraction of the GG gradation does not contain RA. Table 3 summarises the composition by mass of the mixtures in terms of fresh bitumen from the emulsion, aged bitumen from RA aggregate and cement.

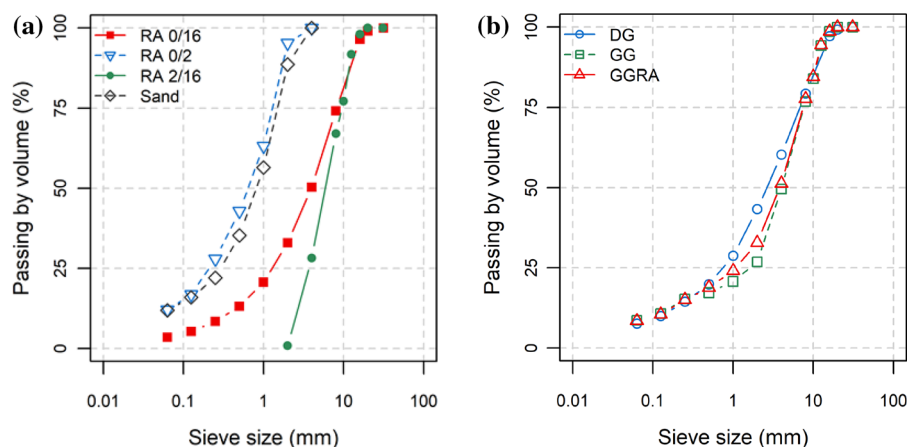
For all mixtures, the emulsion dosage was 5.0% (residual bitumen 3%) and the cement dosage was

2.5% by dry aggregate mass, resulting in a B/C ratio of 1.2. The mixtures can be classified as CBTM according to the scheme proposed in Fig. 1, even though the fresh bitumen dosage is slightly higher than those typically characterising these materials.

The total water dosage, comprising the emulsion water and the pre-wetting water, was 4.5% for the DG gradation and 4.0% for the two gap-graded gradations. The target voids content, which included the volume of air and intergranular water, was 9.0%, comparable to the lower values found in the literature (Table 1). A total of six mixtures was investigated by combining the three gradations (DG, GG, GGRA) and the two cement types (C2, C3). Two replicate specimens (R1 and R2) were tested for each mixture.

### 3.3 Specimen preparation

Before mixing, aggregates were dried until reaching constant mass. Next, a quantity of water equal to the

**Fig. 3** Grading distributions: **a** aggregates, **b** mixtures

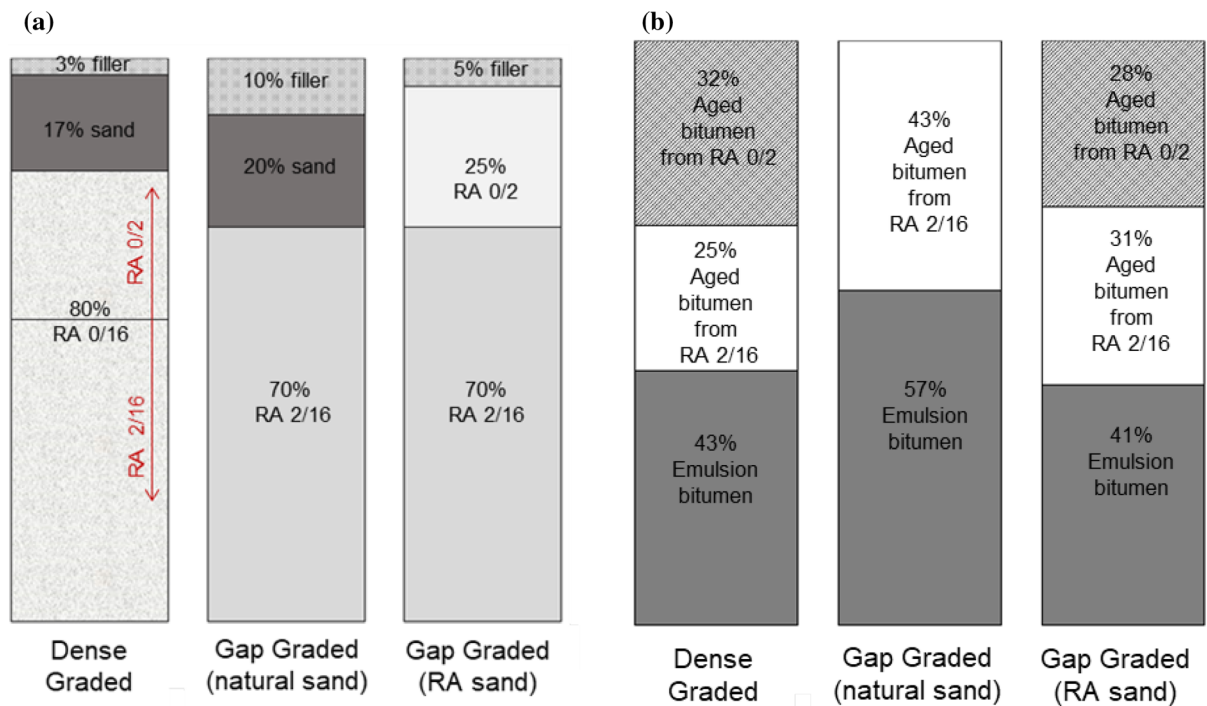


**Fig. 4** Composition of the mixtures: **a** aggregate blend (by dry aggregate mass), **b** bituminous binders (by volume)

**Table 3** Composition of the mixtures in terms of fresh bitumen from emulsion, aged bitumen from RA aggregate and cement (by mixture mass)

ID	Fresh bitumen (%)	Cement (%)	Fresh bitumen / cement (–)	RA bitumen (%)	Total bitumen (%)	RA bitumen / total bitumen (–)
DG	2.7	2.3	1.17	3.6	6.3	0.58
GG	2.7	2.3	1.17	2.1	4.8	0.44
GGRA	2.7	2.3	1.17	4.0	6.7	0.60

water absorption was added to the dry aggregate blend, and the wet samples were sealed in plastic bags for at least 12 h at room temperature to reach the saturated surface dry (SSD) condition. Then, cement, water and bitumen emulsion were gradually added to the SSD aggregate and mixed using a mechanical mixer, alternated with hand-mixing. Immediately after mixing, the specimens were compacted at the target voids content with a gyratory compactor, using a mould with diameter of 150 mm, a pressure of 600 kPa, a gyration speed of 30 rpm and an external angle of gyration of  $1.25^\circ$  (internal angle  $1.16^\circ$ ). The specimens were extracted from the mould right after compaction. Curing was carried out in a climatic chamber for 28 days at  $(25 \pm 2)^\circ\text{C}$  and  $(70 \pm 5)\%$  relative

humidity. At this point, the samples were cored to obtain specimens with a diameter of 75 mm. Then, curing was extended for additional 180 days at  $(25 \pm 2)^\circ\text{C}$  and  $(70 \pm 5)\%$  relative humidity.

### 3.4 Complex modulus testing and rheological modelling

Cyclic uniaxial compression tests were carried out using an AMPT PRO testing system (Fig. 5). The target peak-to-peak strain amplitude was  $30 \cdot 10^{-6}$  mm/mm [34]. The testing frequencies were 10, 5, 1, 0.5 and 0.1 Hz, and twenty loading cycles were applied at each frequency. The sequence of

testing temperatures was 5, 15, 25, 35, 45, 55 °C. The complex modulus  $E^*(\omega)$  was calculated as follows:

$$\begin{aligned} E^*(\omega) &= \frac{\sigma_0}{\varepsilon_0} \exp[j\varphi(\omega)] = E_0(\omega) \exp[j\varphi(\omega)] \\ &= E_1 + jE_2 \end{aligned} \quad (1)$$

where  $\sigma_0$  and  $\varepsilon_0$  are the steady-state amplitudes of the measured stress and strain signals,  $j$  is the imaginary unit,  $\varphi$  is the phase angle, describing the delay of strain with respect to the stress,  $E_0$  is the stiffness modulus,  $E_1$  and  $E_2$  are the storage and loss moduli, respectively.

Thermo-rheologically modelling was carried out starting from the application of the TTSP. The reference temperature  $T_{\text{ref}} = 25$  °C was selected, and the reduced frequency ( $f_r$ ) was calculated using the closed-form shifting (CFS) algorithm based on the minimisation of the overlapping area between two successive isothermal curves of the stiffness modulus  $E_0$  [44]. The temperature dependency of the shift factors ( $a_{T_{\text{ref}}}(T)$ ) was modelled using the Williams–Landel–Ferry (WLF) equation:

$$\log a_{T_{\text{ref}}}(T) = -\frac{C_1(T - T_{\text{ref}})}{C_2 + T - T_{\text{ref}}} \quad (2)$$

where  $C_1$ ,  $C_2$  are constants obtained by least-squares fitting [45].

Rheological modelling of the complex modulus data was carried out with an approach specifically developed for CBTM mixtures. In addition to the viscous dissipation due to the bituminous binding agent, which is normally considered in LVE models, a

hysteretic dissipation component was considered. The model is described as follows:

$$E_{HY}^*(\omega) = E_{LVE}^*(\omega) \cdot \exp[j\varphi_{HY}] \quad (3)$$

where  $E_{LVE}^*$  is the LVE complex modulus model simulating a frequency- and temperature-dependent dissipation and  $\exp(j\varphi_{HY})$  is a correction term that adds a constant phase angle  $\varphi_{HY}$  [31, 34]. Physically,  $\varphi_{HY}$  describes time-independent (non-viscous) and temperature-independent dissipation phenomena which affect the CBTM behaviour during cyclic loading. Hysteretic dissipation is generally used to describe the dynamic behaviour of granular soils or cement concrete [46, 47]. In CBTM mixtures, the hysteretic dissipation may be linked to the presence of cementitious bonds and internal friction caused by an incomplete coating of the aggregate. In the present research the analogical 2S2P1D model [48] was used to simulate the LVE behaviour:

$$E_{LVE}^*(\omega) = E_e + \frac{E_g - E_e}{1 + \delta(j\omega\tau)^{-k} + (j\omega\tau)^{-h} + (j\omega\beta\tau)^{-1}} \quad (4)$$

where  $\omega = 2\pi f_r$  is the angular frequency,  $\delta$ ,  $h$ ,  $k$  and  $\beta$  are binder-related dimensionless shape parameters and  $\tau$  is the characteristic time parameter. The dimensionless parameter  $\beta$  can be written as follows:

$$\beta = \frac{\eta}{\tau(E_g - E_e)} \quad (5)$$

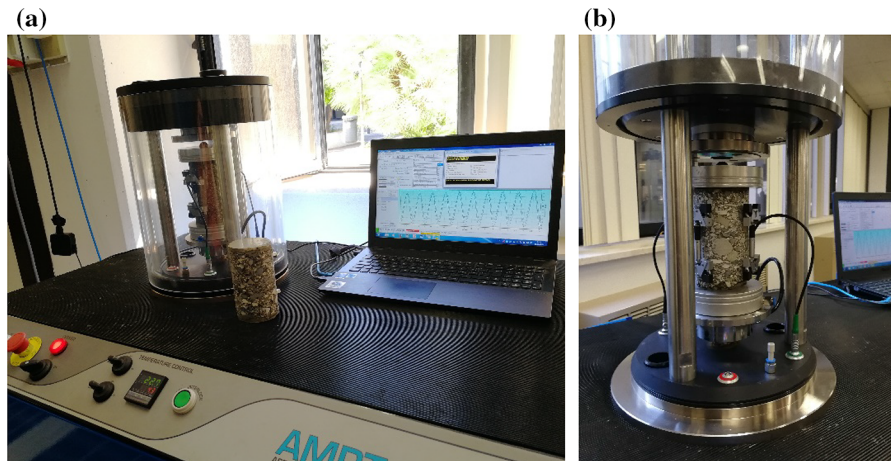


**Fig. 5** Complex modulus testing: **a** AMPT PRO device, **b** detail of the testing configuration

where the parameter  $\eta$  is a Newtonian viscosity parameter used to represent the behaviour of the bituminous binder at very high temperatures [49].

## 4 Results and modelling

### 4.1 Complex modulus results

Figure 6 depicts the complex modulus measurements in the Black and Cole–Cole diagrams. As can be observed, the overall thermo-rheological response followed the typical behaviour of bituminous materials. We measured the highest values of the stiffness modulus at the lowest temperature and highest frequency (5 °C and 10 Hz). For the DG specimens, the average value (standard deviation) was 7533 MPa (1991 MPa), whereas for the GG and GGRA specimens together, we obtained 9340 MPa (2488 MPa). Therefore, the ratio between the average values of  $E_o$  of gap graded and DG specimens was 1.24. On the other hand, we measured the lowest values of the stiffness modulus at the highest temperature and lowest frequency (55 °C and 0.1 Hz). In this condition, the effect of gradation was more evident. In fact, for the DG specimens, we obtained 555 MPa (158 MPa), whereas for the GG and GGRA specimens together, we obtained 1499 MPa (554 MPa), resulting in a ratio between the  $E_o$  values of 2.70. Considering the full testing temperature and frequency range, the gap-graded mixtures were stiffer and showed a lower thermal sensitivity with respect to the dense-graded mixtures (the variability of  $E_o$  across the entire temperature and frequency range was less than one order of magnitude). Based on the composition data shown in Fig. 4 and Table 3, we observe that the difference in stiffness is not related to the bitumen (either fresh or aged) or cement content. However, we can hypothesize that gap-graded mixtures were stiffer because of the higher volume of coarse RA aggregates resulting in an improved stone-on-stone contact. We highlight that the measurements carried out in the present research fall within the stiffness modulus range outlined in Fig. 2.

As regards the phase angle, the lowest values were also measured at 5 °C and 10 Hz. In these conditions, considering all the specimens, the average value (standard deviation) was 5.1° (1.1°). Increasing the

temperature/reducing the frequency, the phase angle increased, reaching a maximum at 45 °C or 55 °C. For the DG specimens, we obtained a maximum of 21.0° (2.4°), whereas for the GG and GGRA specimens together, we obtained 15.5° (2.54°). These maximum values are lower than typical HMA ones [50] because of the lower frequency and thermal sensitivity of CRM mixtures, whose dissipation behaviour is affected by the presence of both the aged RA bitumen and the cementitious bonds. Similar values of the maximum phase angle were also found in the references listed in Table 1.

### 4.2 Modelling

For all tested specimens, the  $(E_o, \varphi)$  and  $(E_1, E_2)$  pairs described unique curves in the Black and Cole–Cole diagrams (Fig. 6). Therefore, we considered the material behaviour to be thermo-rheologically simple and applied the TTSP to obtain the master curves of stiffness modulus and phase angle as a function of the reduced frequency ( $T_{ref} = 25$  °C). Figure 7 shows the calculated temperature shift factors along with the fitted WLF models (Eq. 2). Mixtures DG and GGRA had similar values of  $C_1$  and  $C_2$ , whereas the values for mixture GG were smaller. Practically, for the latter mixture, the slope of the WLF curve was somewhat lower, indicating a lower temperature dependency. Considering the data shown in Table 3, this different thermal sensitivity can be linked to the lower ratio between the aged RA bitumen and the fresh bitumen that characterised the mixtures GG.

Table 4 summarises the corrected 2S2P1D model (herein named 2S2P1D-HY) fitting parameters for all specimens, whereas Fig. 8 shows the fitted model for specimens DG-C3\_R2 and GGRA-C2\_R2 as an example. Figure 8 also shows the effect of the hysteretic correction  $\varphi_{HY}$  by plotting the 2S2P1D model without correction (dashed curves). Both 2S2P1D and 2S2P1D-HY models provide the same, good fitting of the stiffness modulus master curves (Fig. 8c), as the hysteretic correction  $\varphi_{HY}$  produces a rotation in the complex plane, without altering the length of the  $E_o$  vector [18]. On the contrary, it is quite evident that the 2S2P1D-HY model results in an enhanced fitting of the phase angle master curves (Fig. 8d) and the experimental data plotted in the Cole–Cole and Black diagram (Fig. 8a and b). In particular, for the specimen DG-C3\_R2,  $\varphi_{HY}$  was 2.2°,





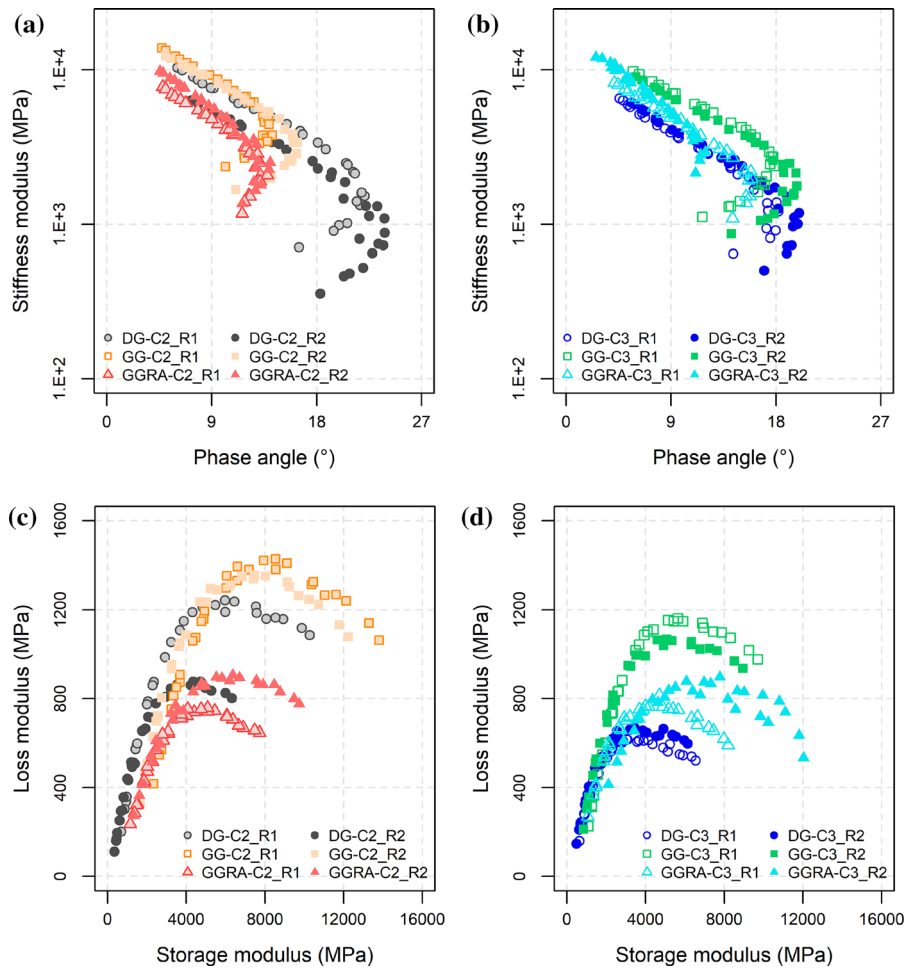


**Fig. 6** Complex modulus results: **a** Black diagram, **b** Cole–Cole diagram

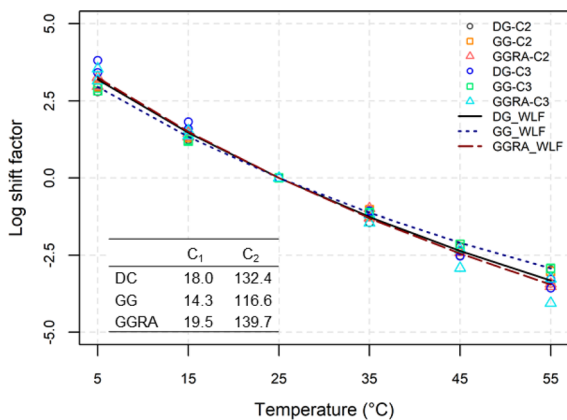


**Fig. 7** Shift factors and WLF model parameters ( $T_{ref} = 25\text{ }^{\circ}\text{C}$ )

corresponding to the 40% and 11% of the minimum and maximum phase angle measurements, respectively. For the specimen GGRA-C2\_R2,  $\varphi_{HY}$  was  $0.9^{\circ}$ , corresponding to the 20% and 6% of the minimum and maximum phase angle measurements, respectively. Thus, although the hysteretic correction was small, at intermediate and low temperatures, it represented a non-negligible part of the phase angle for CBTM mixtures. To give a synthetic overview of the deviation between the measurements and the 2S2P1D-HY model predictions we calculated the following parameters:

$$\Delta E_0 = \frac{E_{0,measured} - E_{0,model}}{E_{0,measured}} \cdot 100 \tag{6a}$$

$$\Delta\varphi = \varphi_{measured} - \varphi_{model} \tag{6b}$$



**Table 4** Parameters of the 2S2P1D-HY rheological model ( $T_{\text{ref}} = 25 \text{ }^{\circ}\text{C}$ )

Specimen	$E_e$ (MPa)	$E_g$ (MPa)	$k$ (-)	$h$ (-)	$\delta$ (-)	$\beta$ (-)	$\log \tau$ (-)	$\varphi_{HY}$ ( $^{\circ}$ )
DG-C2_R1	490	14,990	0.12	0.38	1.75	1905	-0.70	2.7
DG-C2_R2	263	11,150			1.95	1905	-1.62	2.4
DG-C3_R1	450	9310			2.09	1230	-0.15	1.5
DG-C3_R2	370	9096			2.05	851	-0.63	2.2
GG-C2_R1	1995	18,324	0.13	0.40	1.68	488	-0.53	1.8
GG-C2_R2	1407	16,872			1.68	424	-0.74	2.0
GG-C3_R1	895	14,309			1.66	722	-1.02	1.8
GG-C3_R2	750	13,264			1.78	302	-1.05	2.2
GGRA-C2_R1	750	10,323	0.12	0.33	1.72	4259	0.07	1.7
GGRA-C2_R2	799	14,110			1.99	3802	0.05	0.9
GGRA-C3_R1	560	10,571			1.64	5012	0.12	1.6
GGRA-C3_R2	1200	14,923			2.07	4677	1.50	0.5

Adopting the 2S2P1D-HY model,  $\Delta E_0$  values were generally lower than 10% (Fig. 9a) and  $\Delta\varphi$  values were generally lower than  $3^{\circ}$  (Fig. 9b), confirming the good accuracy of the fitting. Due to the hysteretic correction, we also observe that, at  $f_r$  higher than 0.1 Hz, the 2S2P1D-HY model predicted the phase angle with an error lower than  $1^{\circ}$ .

## 5 Discussion

First, we investigate the link between the rheological parameters listed in Table 4 and the composition of the mixtures described in Fig. 4 and Table 3. Considering all the specimens, the hysteretic correction  $\varphi_{HY}$  varied from  $0.5^{\circ}$  to  $2.7^{\circ}$  and, on average, specimens DG and GG were characterised by higher values with respect to specimens GGRA. Mixtures DG and GG also had a lower total bitumen content (fresh + aged). This confirms that  $\varphi_{HY}$  is linked to dissipation mechanisms that are not related to the bituminous component of the mixtures and thus are frequency and temperature-independent.

The gradation of the mixtures had a clear effect on the equilibrium and glassy moduli, and thus on the elastic component of the rheological behaviour. In particular, GG and GGRA specimens had higher values of  $E_e$ , which could be related to an improved stone-to-stone contact in the gradation. Moreover, the GG specimens were characterised, on average, by the

highest values of  $E_e$  and  $E_g$ . In terms of composition, the GG mixtures were characterised by a fine aggregate matrix (FAM) containing only virgin sand (no RA). This favoured the development of cementitious bonds within the FAM, leading to higher stiffness at all temperatures and frequencies. The DG specimens were also characterised by the lowest values of  $E_e$ . Since the equilibrium modulus is linked to the properties of the aggregate skeleton, this highlights the stiffening role played by the coarse stone-on-stone contact, which is prevalent in the gap-graded gradations GG and GGRA. The values of  $E_e$  and  $E_g$  were also affected by the cement type. In fact, with the same gradation, the mixtures produced with cement C2 were generally stiffer than those produced with cement C3. This is particularly evident for mixtures GG that, as highlighted above, were characterised by a cement-dominated FAM.

The parameters  $h$ ,  $k$ ,  $\delta$  and  $\beta$  of the 2S2P1D model are linked to the LVE response of the bituminous component of the mixtures that, in the present case, comprises both fresh emulsion bitumen and aged RA bitumen. In particular,  $h$  and  $k$  must be comprised between 0 and 1, with lower values representing a more elastic behaviour and higher values representing a more viscous behaviour. In our model fitting, we used the same values of  $h$  (0.38, 0.40 and 0.33) and  $k$  (0.12, 0.13 and 0.12) for specimens characterised by the same gradation (DG, GG, GGRA, respectively), and thus by the same bitumen content. Even though the values of  $h$  and  $k$  were not specifically optimised

for each specimen, a good precision was obtained (Fig. 9). As shown in Fig. 10a, the values of  $h$  and  $k$  found in the present research were similar to those obtained for other CRM mixtures [30, 31, 34] but significantly lower than those commonly obtained for conventional hot and hot-recycled asphalt mixtures [48, 49]. This suggests that the RA binder affects the rheological behaviour of CRM mixtures by reducing the values of  $h$  and  $k$ , but with a different mechanism than in hot recycled mixtures. We highlight that this phenomenological interpretation does not imply any reactivation of the aged RA binder nor its blending with the emulsion residue. In fact, cold recycling is carried out at ambient temperature, where the RA binder is still viscoelastic but can hardly be considered

“active”. Neither it can be assumed that the RA binder significantly blends with the emulsion residue, generating a new “reactivated” binder. Figure 10b shows the relation between the characteristic time  $\tau$  and the Newtonian viscosity parameter  $\eta$ . Specimens GGRA had the highest values of both  $\tau$  and  $\eta$  indicating lower viscous relaxation ability and higher ageing degree with respect to the mixtures DG and GG. This result can also be linked to the content of aged binder in the mixtures (Table 3).

Figure 11 compares the measured stiffness modulus values with the range of data obtained from the literature review (Fig. 2a, Table 1). At high reduced frequencies ( $f_r = 10^6$  Hz), the tested mixtures had stiffness modulus values comparable to those of the

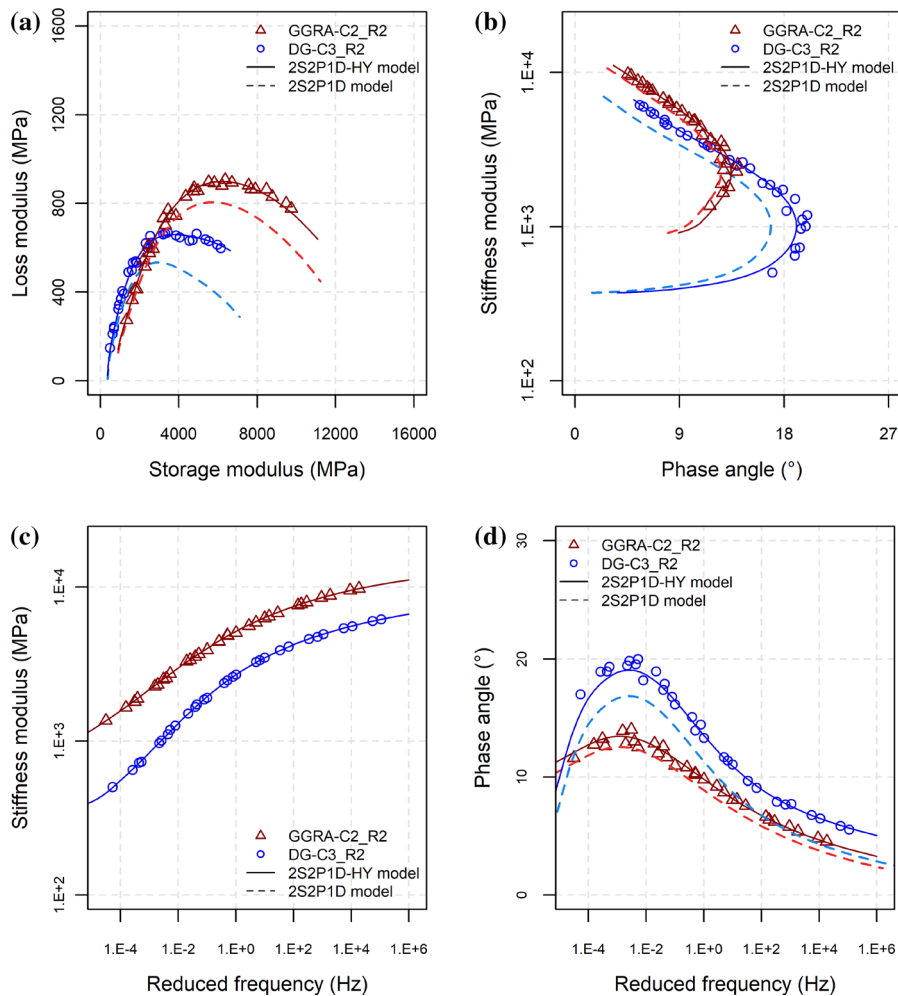


**Fig. 8** Examples of complex modulus results and rheological modelling: **a** Cole–Cole diagram; **b** Black diagram, **c** stiffness modulus master curves; **d** phase angle master curves

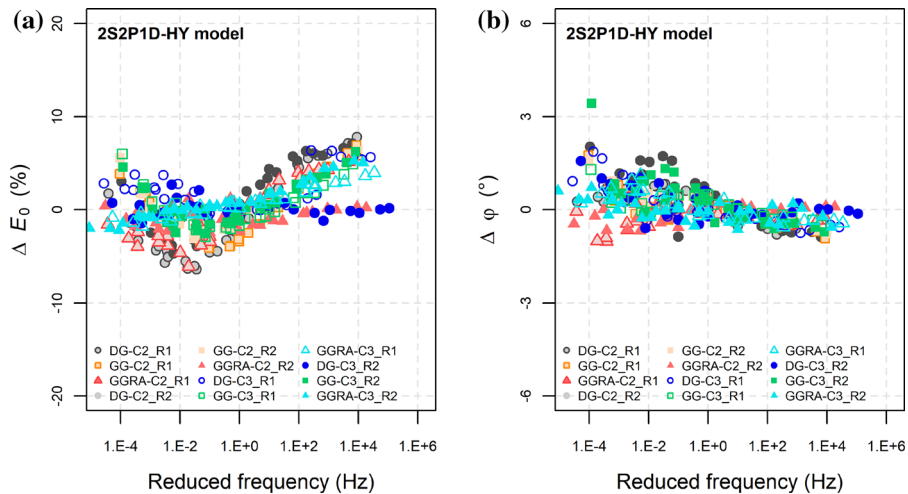


**Fig. 9** Accuracy of the fitted 2S2P1D-HY model: **a** stiffness modulus, **b** phase angle

mixtures considered in the literature review. In particular, the values of  $E_0(10^6)$  varied from 6660 to 14,910 MPa, whereas the literature data varied from 6625 to 18,230 MPa. On the other hand, at low reduced frequencies ( $f_r = 10^{-4}$  Hz), the stiffness modulus  $E_0(10^{-4})$  of the tested mixtures was comprised between 343 and 2920 MPa. In contrast, the literature data varied from 66 to 2356 MPa. This suggests that the use of high-strength cements in relatively high dosage (2.5%) did not lead to an excessive stiffness at low temperatures that could result in a cracking-prone behaviour. On the other hand, the material was still quite stiff at high temperatures suggesting a good permanent

deformation resistance. However, we highlight that these results refer to the small-strain behaviour and extrapolation to the failure behaviour must be supported by specific experiments.

### 6 Conclusions

In this paper we evaluated the effect of different grading curves, RA contents and cement types on the complex modulus behaviour of CBTM mixtures. The analysis of experimental data was based on a rheological modelling approach specifically developed for CBTM mixtures, which considers also a hysteretic

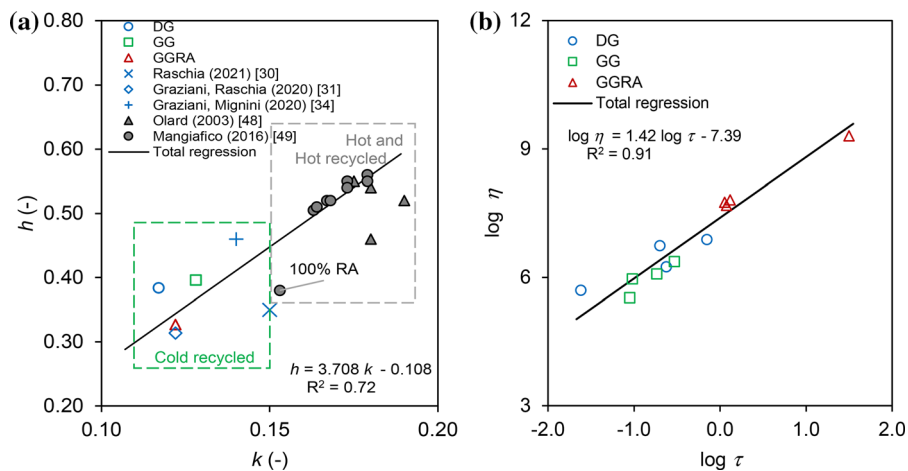


**Fig. 10** Relation between the parameters of the rheological model: **a**  $k$  and  $h$  values; **b**  $\tau$  and  $\eta$  values



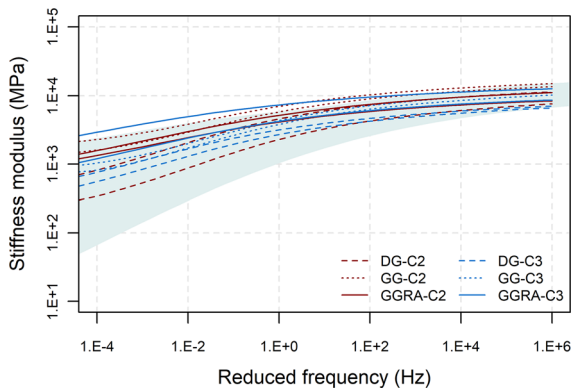


**Fig. 11** Stiffness modulus master curves (2S2P1D-HY model) of the investigated mixtures superposed to the master curves envelope of CRM mixtures from the literature review

dissipation mechanism. The main findings can be summarised as follows:

- Gap-graded gradations lead to a stiffness increase, especially at high temperatures with respect to dense graded gradations. This is due to a higher number of coarse stone-to-stone contact points.
- The cement type affects the elastic component of the rheological behaviour, and in particular, the values of the asymptotic moduli  $E_e$  and  $E_g$ . This effect is particularly evident in the mixtures with a cement-dominated FAM.
- The 2S2P1D-HY model allows an excellent fitting of the complex modulus results and the hysteretic correction angle  $\phi_{HY}$  is higher for mixtures having lower bitumen content (fresh + aged) confirming that  $\phi_{HY}$  is linked to dissipation mechanisms that are frequency and temperature-independent.
- CBTM mixtures are characterised by values of the rheological parameters  $h$  and  $k$  that are well below those of hot recycled mixtures. This could be related to the fact that in cold recycling, contrary to hot recycling, the fresh bituminous binder and the aged RA binder do not blend.

**Author contributions** The authors confirm contribution to the paper as follows: Study conception and design: A. Graziani, C. Mignini; Data collection: C. Mignini; Analysis and interpretation of results: C. Mignini, A. Graziani, F Cardone; Draft manuscript preparation: C. Mignini, A. Graziani, F. Cardone; Supervision: A. Graziani. All authors reviewed the results and approved the final version of the manuscript.

**Funding** Open access funding provided by Università Politecnica delle Marche within the CRUI-CARE Agreement.

#### Declarations

**Conflict of interest** The authors have no relevant financial or non-financial interests to disclose.

**Open Access** This article is licensed under a Creative Commons Attribution 4.0 International License, which permits use, sharing, adaptation, distribution and reproduction in any medium or format, as long as you give appropriate credit to the original author(s) and the source, provide a link to the Creative Commons licence, and indicate if changes were made. The images or other third party material in this article are included in the article's Creative Commons licence, unless indicated otherwise in a credit line to the material. If material is not included in the article's Creative Commons licence and your intended use is not permitted by statutory regulation or exceeds the permitted use, you will need to obtain permission directly from the copyright holder. To view a copy of this licence, visit <http://creativecommons.org/licenses/by/4.0/>.

#### References

1. European Commission (2020) Circular economy action plan. doi:<https://doi.org/10.2779/717149>
2. Del Carmen Rubio M, Moreno F, Martínez-Echevarría MJ, Martínez G, Vázquez JM (2013) Comparative analysis of emissions from the manufacture and use of hot and half-warm mix asphalt. J Clean Prod. <https://doi.org/10.1016/j.jclepro.2012.09.036>
3. D'Angelo J et al (2008) Warm-mix asphalt: European practice. Washington, DC, United States. No. FHWA-PL-08-007
4. Thenoux G, González Á, Dowling R (2007) Energy consumption comparison for different asphalt pavements rehabilitation techniques used in Chile. Resour Conserv Recycl 49(4):325–339. <https://doi.org/10.1016/j.resconrec.2006.02.005>
5. Cross S, Chesner W, Justus H, Kearney E (2011) Life-cycle environmental analysis for evaluation of pavement rehabilitation options. Transp Res Rec. <https://doi.org/10.3141/2227-05>
6. Giani MI, Dotelli G, Brandini N, Zampori L (2015) Comparative life cycle assessment of asphalt pavements using reclaimed asphalt, warm mix technology and cold in-place recycling. Resour Conserv Recycl. <https://doi.org/10.1016/j.resconrec.2015.08.006>
7. Xiao F, Yao S, Wang J, Li X, Amirkhanian S (2018) A literature review on cold recycling technology of asphalt pavement. Constr Build Mater 180:579–604. <https://doi.org/10.1016/j.conbuildmat.2018.06.006>
8. Raschia S, Perraton D, Graziani A, Carter A (2020) Influence of low production temperatures on compactability and mechanical properties of cold recycled mixtures. Constr Build Mater. <https://doi.org/10.1016/j.conbuildmat.2019.117169>

9. Nassar AI, Mohammed MK, Thom N, Parry T (2018) Characterisation of high-performance cold bitumen emulsion mixtures for surface courses. *Int J Pavement Eng*. <https://doi.org/10.1080/10298436.2016.1176165>
10. Bocci M, Grilli A, Cardone F, Graziani A (2011) A study on the mechanical behaviour of cement-bitumen treated materials. *Constr Build Mater* 25(2):773–778. <https://doi.org/10.1016/j.conbuildmat.2010.07.007>
11. Valentin J, Čížková Z, Suda J, Batista F, Mollenhauer K, Simnofske D (2016) Stiffness characterization of cold recycled mixtures. *Transp Res Procedia* 14:758–767. <https://doi.org/10.1016/j.trpro.2016.05.065>
12. Dolzycki B, Jaczewski M, Szydłowski C (2017) The long-term properties of mineral-cement-emulsion mixtures. *Constr Build Mater* 156:799–808. <https://doi.org/10.1016/j.conbuildmat.2017.09.032>
13. Raschia S, Mignini C, Graziani A, Carter A, Perraton D, Vaillancourt M (2019) Effect of gradation on volumetric and mechanical properties of cold recycled mixtures (CRM). *Road Mater Pavement Des* 20(sup2):S740–S754. <https://doi.org/10.1080/14680629.2019.1633754>
14. Zhu C, Zhang H, Huang L, Wei C (2019) Long-term performance and microstructure of asphalt emulsion cold recycled mixture with different gradations. *J Clean Prod* 215:944–951. <https://doi.org/10.1016/j.jclepro.2019.01.103>
15. Mignini C, Virgili A, Graziani A (2022) On the densification of cold recycled asphalt mixtures. *J Test Eval*. <https://doi.org/10.1520/JTE20210306>
16. Xu O, Wang Z, Wang R (2017) Effects of aggregate gradations and binder contents on engineering properties of cement emulsified asphalt mixtures. *Constr Build Mater*. <https://doi.org/10.1016/j.conbuildmat.2016.12.095>
17. Mignini C, Cardone F, Graziani A (2020) Mechanical behaviour of cold recycled asphalt mixtures for binder courses produced with bitumen emulsion and high strength cement. In: Proceedings of the 9th international conference on maintenance and rehabilitation of pavements—Mair-epav9, pp 365–374
18. Ferrotti G, Grilli A, Mignini C, Graziani A (2020) Comparing the field and laboratory curing behaviour of cold recycled asphalt mixtures for binder courses, pp 12–14. doi:<https://doi.org/10.3390/ma13214697>
19. Solaimanian M, Chen X, Tavassoti-Kheiry P, Milander S (2017) Performance of RAP cold mixes with polymer modified emulsions, no. July 2016, pp 1–16
20. Jiang J, Ni F, Zheng J, Han Y, Zhao X (2020) Improving the high-temperature performance of cold recycled mixtures by polymer-modified asphalt emulsion. *Int J Pavement Eng* 21(1):41–48. <https://doi.org/10.1080/10298436.2018.1435882>
21. Fang X, Garcia A, Winnefeld F, Partl MN, Lura P (2016) Impact of rapid-hardening cements on mechanical properties of cement bitumen emulsion asphalt. *Mater Struct Constr* 49(1–2):487–498. <https://doi.org/10.1617/s11527-014-0512-3>
22. Saadoon T, Gómez-Mejide B, Garcia A (2018) Prediction of water evaporation and stability of cold asphalt mixtures containing different types of cement. *Constr Build Mater* 186:751–761. <https://doi.org/10.1016/j.conbuildmat.2018.07.218>
23. Mignini C, Cardone F, Graziani A (2021) Using fine aggregate matrix mortars to predict the curing behaviour of cement bitumen treated materials produced with different cements. *Constr Build Mater* 268:121201. <https://doi.org/10.1016/j.conbuildmat.2020.121201>
24. Mollenhauer K et al (2020) Deliverable D5—International pavement designs with cold recycled material. Proposal of pavement design procedure including structure catalogue and identification of failure modes for MEPD,” CRABfor-OERE, CEDR Call, [Online]. Available: <https://www.crabforoere.eu/project-reports/>
25. Fedrigo W, Núñez WP, Visser AT (2020) A review of full-depth reclamation of pavements with Portland cement: Brazil and abroad. *Constr Build Mater* 262:120540. <https://doi.org/10.1016/j.conbuildmat.2020.120540>
26. Asphalt Academy, Technical Guideline TG2: Bitumen Stabilised Materials: A Guideline for the Design and Construction of Bitumen Emulsion and Foamed Bitumen Stabilised Materials, 3rd edition. Pretoria, South Africa: Asphalt Academy, 2020.
27. Orosa P, Pérez I, Pasandín AR (2021) Short-term resilient behaviour and its evolution with curing in cold in-place recycled asphalt mixtures. *Constr Build Mater* 323(April):2022. <https://doi.org/10.1016/j.conbuildmat.2022.126559>
28. Redelius P, Östlund JA, Soenen H (2016) Field experience of cold mix asphalt during 15 years. *Road Mater Pavement Des* 17(1):223–242. <https://doi.org/10.1080/14680629.2015.1068702>
29. Day D, Lancaster IM, McKay D (2019) Emulsion cold mix asphalt in the UK: a decade of site and laboratory experience. *J. Traffic Transp. Eng. (English Ed.)* 6(4):359–365
30. Raschia S, Perraton D, Di Benedetto H, Lamothe S, Graziani A, Carter A (2021) Visco-elasto-plastic characterization in the small strain domain of cement-bitumen treated materials produced at low temperatures. *J Mater Civ Eng* 33(4):04021039. [https://doi.org/10.1061/\(ASCE\)MT.1943-5533.0003653](https://doi.org/10.1061/(ASCE)MT.1943-5533.0003653)
31. Graziani A, Raschia S, Mignini C, Carter A (2020) Use of fine aggregate matrix to analyze the rheological behavior of cold recycled materials. *Mater. Struct.* 7:5. <https://doi.org/10.1617/s11527-020-01515-7>
32. Mehranfar V, Modarres A (2020) Evaluating the recycled pavement performance and layer moduli at variable temperature by nondestructive tests. *Int J Pavement Eng* 21(7):817–829. <https://doi.org/10.1080/10298436.2018.1511784>
33. Schwartz CW, Diefenderfer BK, Bowers BF (2017) Material properties of cold in-place recycled and full-depth reclamation asphalt concrete
34. Graziani A, Mignini C, Bocci E, Bocci M (2020) Complex modulus testing and rheological modeling of cold-recycled mixtures. *J Test Eval* 48(1):20180905. <https://doi.org/10.1520/jte20180905>
35. Cardone F, Grilli A, Bocci M, Graziani A (2015) Curing and temperature sensitivity of cement-bitumen treated materials. *Int J Pavement Eng* 16(10):868–880. <https://doi.org/10.1080/10298436.2014.966710>
36. Godenzoni C, Graziani A, Perraton D (2017) Complex modulus characterisation of cold-recycled mixtures with foamed bitumen and different contents of reclaimed asphalt.



- Road Mater Pavement Des 18(1):130–150. <https://doi.org/10.1080/14680629.2016.1142467>
37. Gandhi A, Carter A, Singh D (2017) Rheological behavior of cold recycled asphalt materials with different contents of recycled asphalt pavements. *Innov Infrastruct Solut* 2(1):1–9. <https://doi.org/10.1007/s41062-017-0094-3>
  38. Lin J, Hong J, Xiao Y (2017) Dynamic characteristics of 100% cold recycled asphalt mixture using asphalt emulsion and cement. *J Clean Prod*. <https://doi.org/10.1016/j.jclepro.2017.04.065>
  39. Buczyński P, Iwański M (2018) Complex modulus change within the linear viscoelastic region of the mineral-cement mixture with foamed bitumen. *Constr Build Mater*. <https://doi.org/10.1016/j.conbuildmat.2018.03.214>
  40. Graziani A, Godenzoni C, Canestrari F (2019) Experimental characterization of the 3D linear viscoelastic behavior of cold recycled bitumen emulsion mixtures. *J Traffic Transp Eng (English Ed)*. <https://doi.org/10.1016/j.jtte.2019.03.001>
  41. Kuchiishi AK, Vasconcelos K, Bariani Bernucci LL (2019) Effect of mixture composition on the mechanical behaviour of cold recycled asphalt mixtures. *Int J Pavement Eng*. <https://doi.org/10.1080/10298436.2019.1655564>
  42. Autostrade per l'Italia (2013) Norme tecniche di appalto pavimentazioni
  43. Provincia Autonoma di Bolzano (2016) Capitolato speciale d'appalto opere stradali
  44. Gergesova M, Zupančič B, Saprunov I, Emri I (2011) The closed form t-T-P shifting (CFS) algorithm. *J. Rheol.* 55(1):1–16. <https://doi.org/10.1122/1.3503529>
  45. Ferry JD (1980) Viscoelastic properties of polymers
  46. Ashmawy AK, Salgado R, Guha S, Drnevich VP (1995) Soil damping and its use in dynamic analyses. In: Third international conferences recent advances in geotechnical earthquake engineering soil dynamics 1-static dynamics. *Eng. Soil Parameters Const. Relations Soils*
  47. Genta G, Keith RH (2009) Vibration dynamics and control. *Noise Control Eng J*. <https://doi.org/10.3397/1.3110987>
  48. Olard F, Di Benedetto H (2003) General '2S2P1D' model and relation between the linear viscoelastic behaviours of bituminous binders and mixes. *Road Mater Pavement Des* 4(2):185–224. <https://doi.org/10.1080/14680629.2003.9689946>
  49. Mangiafico S, Di Benedetto H, Sauzéat C, Olard F, Pouget S, Planque L (2016) Effect of colloidal structure of bituminous binder blends on linear viscoelastic behaviour of mixtures containing Reclaimed Asphalt Pavement. *Mater Des* 111:126–139. <https://doi.org/10.1016/j.matdes.2016.07.124>
  50. Kim YR (2009) Modeling of asphalt concrete

**Publisher's Note** Springer Nature remains neutral with regard to jurisdictional claims in published maps and institutional affiliations.

